

# Study of Cyclization of Diphenylacetals Derived from L-rhamnose and L-fucose: A Theoretical Approach

A.E. Bañuelos-Hernández<sup>a</sup> and J.A. Mendoza-Espinoza<sup>b,\*</sup><sup>a</sup>Departamento de Farmacología, Centro de Investigación y de Estudios Avanzados del Instituto Politécnico Nacional, México D.F.<sup>b</sup>Laboratorio de Productos Naturales. Academia de Biología Humana, Colegio de Ciencia y Tecnología, Universidad Autónoma de la Ciudad de México, México D.F.

Received 18 October 2011, revised 20 February 2012, accepted 22 March 2012.

## ABSTRACT

This work aimed to study the configuration of two mono-tosyl-diphenylacetals, highly flexible molecules derived from L-rhamnose and L-fucose, by means of the Monte Carlo conformational search method. The energy of the conformers established by this method and calculated by using the molecular mechanics force field (MMFF) permitted to establish a first conformational space. The geometry of the conformers was optimized by using the semi-empirical AM<sub>1</sub> and the density functional B3LYP/DGDZVP methods. We were able to explain the different final products recovered from the reaction of the diphenylacetals derived from L-rhamnose and L-fucose with tosyl chloride, in a pyridine solution. On the other hand, obtaining cyclical compounds by intramolecular cyclization could be an attractive pathway for the synthesis of furanosides.

## KEYWORDS

Molecular modelling, conformational analysis, Monte Carlo conformational search method, L-rhamnose, L-fucose, B3LYP, DGDZVP, diphenylthioacetal.

## 1. Introduction

Natural products are compounds with complicated chemical structures, most of which have various chiral centres, such as 6-heptenyl-5,6-dihydro-2H-pyran-2-ones. Several strategies are commonly utilized in order to determine the stereochemical centres of these types of molecules, the analysis by anomalous X-ray diffraction being one of the most accurate methods. More recently, studies utilizing computational methods in combination with nuclear magnetic resonance (NMR) have been used with good results for the determination of stereochemistry and for conformation analysis.<sup>1–4</sup> These latter require a smaller sample and are not limited by the quality of the crystal.

The stereochemistry and conformation of chemical molecules can be used in order to determine chemical properties such as reactivity. In the case of bioactive compounds, chemical reactivity is frequently associated with pharmacological activity. This explains the importance of ascertaining the conformation of these substances and relating it to their chemical reactivity. Furthermore, if the target receptors are known, the application of these kind of studies enables to detect possible interactions that reveal the action mechanism by means of molecular recognition studies.<sup>5–6</sup>

The 6-heptenyl-5,6-dihydro-2H-pyran-2-ones, such as spicigerolide, hyptolide, hypurticin, anamarine, pectinolides A–C, etc., are chemicals isolated from plants of the genus *Hyptis* of the Lamiaceae family.<sup>7–10</sup> These chemical compounds have shown several pharmacological properties, among others cytotoxicity.<sup>11–12</sup> The mechanism of action of the cytotoxicity is thought to be a Michael-type addition to the  $\alpha$ - $\beta$  unsaturated system, which has been demonstrated with molecular biology techniques in the case of pironetin.<sup>13–14</sup> It has been proven that modifications in the spatial arrangement of the side chain of spicigerolide cause changes in the half maximal inhibitory

concentration (IC<sub>50</sub>).<sup>12</sup> Notwithstanding ample evidence available from the pharmacological field, there is a lack of investigations that relate spatial conformation with chemical reactivity, a connection that often determines the pharmacological properties of bioactive substances.

Diphenylthioacetals compounds **2** and **6**, derived from L-fucose (**1**) and L-rhamnose (**5**), are interesting to study because they are intermediaries of cytotoxic compounds of the type of the 6-heptenyl-5,6-dihydro-2H-pyran-2-ones. Compounds **2** and **6** exhibit different chemical behaviour when they react with tosyl chloride, due to their highly flexible structures. Novel molecular modelling techniques can be applied in order to explain their different reactivities. Thus, the purpose of this study was to explain this different behaviour by employing molecular modelling techniques that can be used in order to elucidate reactivity in other complex systems.

## 2. Experimental

### 2.1. Molecular Modelling

The molecular modelling was carried out by employing the Monte Carlo method in combination with the MMFF force field for the search of conformers. The starting conformers are shown in Fig. 1a and Fig. 1b. The selected conformers were situated within an interval of maximum difference 10 kcal mol<sup>-1</sup> from the minimum energy conformer. The chosen conformations were geometrically optimized by employing the semi-empirical method AM1, using the computer program Spartan'04. The modelled structures inside the 10 kcal mol<sup>-1</sup> cut-off value were geometrically optimized. Thermo-chemical and vibrational properties were calculated with the density functional theory using the method B3LYP and the basis DGDZV as implemented in the Gaussian 03W computer package. The results from the three calculus levels (MMFF, AM1, DFT/B3LYP/DGDZVP) were compared. The participation of the conformers in the equilib-

\*To whom correspondence should be addressed.  
E-mail: [amendozaespinoza@gmail.com](mailto:amendozaespinoza@gmail.com) / [josealberto.mendoza@uacm.edu.mx](mailto:josealberto.mendoza@uacm.edu.mx)

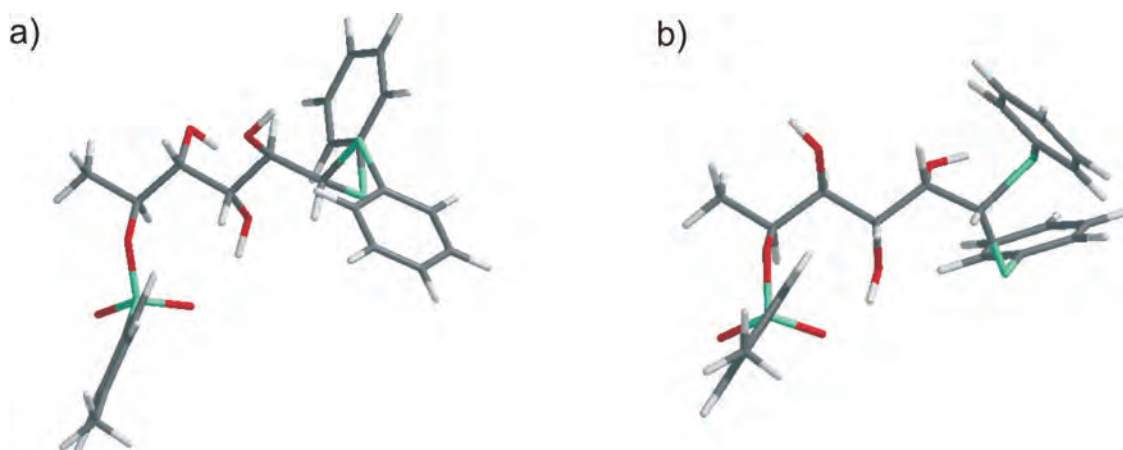


**Figure 1** Starting models of the conformational space sampling using the Monte Carlo method; (a) proposed intermediary 7 and (b) obtained from L-fucose 3.

rium was calculated based in the method previously described for the cases of hypurticine and hypotolide.<sup>2</sup>

To validate the conformer distribution, the magnetic shielding tensors were calculated with the gauge-including atomic orbital (GIAO) method, followed by theoretical calculation of the total NMR spin-spin coupling constants (SSCC) at the B3LYP/DGDZVP level. The  $\Delta G = -RT \ln K$  equation was used to obtain the population for each conformer, taking into consideration a cyclic equilibrium among the selected conformers. Each spin-spin coupling value was Boltzmann-weighted taking into account the DFT population to integrate the population-averaged coupling constants.<sup>15,16</sup>

## 2.2. Preparation of the Diphenyl-dithiols (2 and 6) Derived from L-rhamnose (5) and L-fucose (1)

The diphenyl-dithiols were prepared as shown in Fig. 2, following the methodology described by Frago-Serrano in 2001.<sup>1</sup> Their chemical structure was corroborated by spectral comparison.

## 2.3. 5-Monosulfonyl-diphenyl-dithioacetal Derived from L-fucose (3)

A solution of diphenyl-dithiol 2 was reacted with *p*-toluen-

sulfonyl chloride in pyridine for 48 hours at 4 °C. After this time, the reaction mixture was poured over ice and extracted with AcOEt. It was washed three times with HCl (10 %), a saturated solution of KHCO<sub>3</sub> and saline solution at 1 %, and the solvent removed with a rotary evaporator. It was purified by using a glass column with a diameter of 2 cm, packed with 100 g silica gel, 230–400 mesh. A mixture 97:3 of CH<sub>2</sub>Cl<sub>2</sub>-CH<sub>3</sub>OH was used as mobile phase ( $R_f = 0.6$  in CH<sub>2</sub>Cl<sub>2</sub>-CH<sub>3</sub>OH 9:1). A white powder was obtained (mp = 130–135 °C). <sup>1</sup>H-NMR (300 MHz, CDCl<sub>3</sub>)  $\delta$  7.82 (2H, m, 2 H-4'), 7.50–7.26 (8H, m), 5.25 (1H, 2qt,  $J_{5,6} = 6.6$ ;  $J_{4,5} = 1.0$  Hz, H-5), 4.20 (1H, d,  $J_{1,2} = 7.9$  Hz, H-1), 4.45 (1H, dd,  $J_{2,3} = \delta 1.4$ ,  $J_{3,4} = 9.3$  Hz, H-3), 3.90 (1H, t,  $J_{1,2} = 7.9$  Hz,  $J_{2,3} = 1.4$  Hz, H-2), 3.59 (1H, dd,  $J_{3,4} = 9.3$  Hz,  $J_{4,5} = 1.0$  Hz, H-4), 2.42 (3H, s, CH<sub>3</sub>), 2.30 (3H, as, OH), 1.32 (3H, d,  $J_{5,6} = 6.6$  Hz, H-6). <sup>13</sup>C-RMN (75.4 MHz, CDCl<sub>3</sub>)  $\delta$  144.9 (C), 133.5 (C), 133.3 ( $\times 2$  C), 132.5 ( $\times 2$  C), 132.4 ( $\times 2$  C), 129.0 ( $\times 2$  C), 128.9 ( $\times 2$  C), 127.8 (C), 127.7 ( $\times 2$  C), 78.2 (1 C, C-5), 73.9 (1 C, C-4), 70.8 (1 C, C-2), 69.2 (1 C, C-3), 63.8 (1 C, C-1), 21.9 (1 C, SO<sub>3</sub>C<sub>6</sub>H<sub>4</sub>CH<sub>3</sub>), 17.7 (1 C, CH<sub>3</sub>). EM-IE  $m/z$  365 [M - C<sub>7</sub>H<sub>7</sub>SO<sub>2</sub>] (1), 349 [M - C<sub>7</sub>H<sub>7</sub>SO<sub>3</sub>] (4).

## 2.4. Preparation of the Diphenyl-dithioacetal of 2,5-Anhydro-6-deoxy-L-glucose (8)

A solution of the diphenyl-dithiol 6 (58 mg in pyridine (1.5 mL)

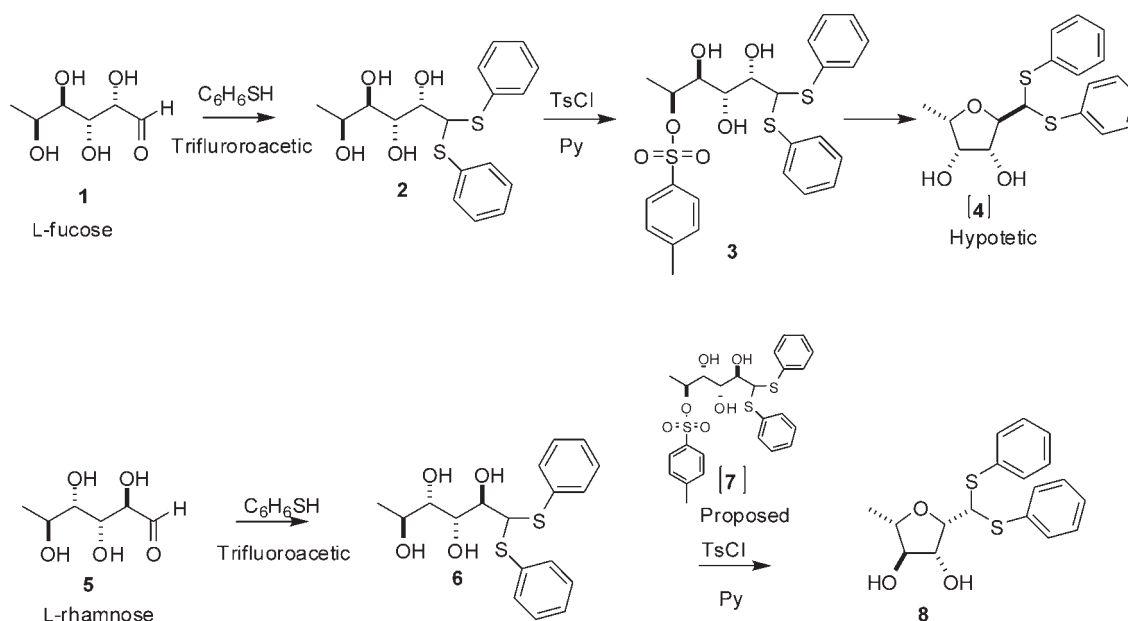


**Figure 2** Reaction scheme of carbohydrates L-fucose (1) and L-rhamnose (5) in presence of tosyl chloride and pyridine.

**Table 1** Minimum energy conformers of derivate 3 of L-fucose (1) obtained by the Monte Carlo method and MMFF, then optimized by employing the semi-empirical calculation base AM1 and DFT method B3LYP/DGDZVP, the global minima of each theory level distribution is in italics.

Conformer	$E_{\text{MMFF}}/\text{kcal mol}^{-1}$	$P_{\text{MMFF}}$	$E_{\text{AM1}}/\text{kcal mol}^{-1}$	$P_{\text{AM1}}$	$E_{\text{DFT}}/\text{kcal mol}^{-1}$	$P_{\text{DFT}}$
3-I	126.0415	0.0002	-193.0589	0.3949	-1640946.5280	0.4648
3-II	128.0277	0.0000	-192.9978	0.3562	-1640946.4715	0.4226
3-III	126.4473	0.0001	-192.7021	0.2163	-1640945.0671	0.0395
3-IV	122.0458	0.1386	-190.9153	0.0106	-1640944.9956	0.0350
3-V	127.5487	0.0000	-191.2440	0.0185	-1640944.9561	0.0328
3-VI	127.0017	0.0000	-190.1765	0.0031	-1640943.8705	0.0052
3-VII	120.9677	0.8545	-188.8808	0.0003	-1640941.1082	0.0000
3-VIII	123.9146	0.0059	-186.2147	0.0000	-1640940.7718	0.0000
3-IX	125.3852	0.0005	-186.5085	0.0000	-1640938.4777	0.0000
3-X	126.2044	0.0001	-186.4069	0.0000	-1640937.6776	0.0000
3-XI	126.4534	0.0001	-188.0008	0.0001	-1640935.7436	0.0000
3-XII	127.8713	0.0000	-184.5755	0.0000	-1640935.1425	0.0000

was reacted in equimolecular proportions with *p*-toluenesulfonyl chloride (60 mg in 1.5 mL pyridine for 48 hours at 4 °C. After this time, the reaction mixture was poured over ice and extracted with AcOEt. It was washed three times with HCl (10 %), saturated solution of KHCO<sub>3</sub> and saline solution at 1 %. The solvent was removed with a rotary evaporator and purified by using a glass column with a diameter of 2 cm, packed with 100 g of 230–400 mesh silica gel. A mixture 97:3 of CH<sub>2</sub>Cl<sub>2</sub>-CH<sub>3</sub>OH was used as mobile phase. Fractions of 10 mL were collected. The product was obtained as a solid from fractions 32–44, with an approximate yield of 81 % (44.5 mg, mp 135–140)C, R<sub>f</sub> = 0.7 in CH<sub>2</sub>Cl<sub>2</sub>-CH<sub>3</sub>OH 9:1. ORD (c 0.26, MeOH) [ $\alpha$ ]<sub>589</sub> = 1.2°, [ $\alpha$ ]<sub>578</sub> = 1.2°, [ $\alpha$ ]<sub>546</sub> = 1.2], [ $\alpha$ ]<sub>436</sub> = 2.7°, [ $\alpha$ ]<sub>365</sub> = 3.5°. IR (MeOH)  $\nu_{\text{max}}$  3602 (OH), 3424 (OH), 1582 (C<sub>6</sub>H<sub>5</sub>), 1084 cm<sup>-1</sup> (C-O). UV (EtOH)  $\lambda_{\text{max}}$  (log  $\epsilon$ ) 218 (3.75), 257 nm (3.52). <sup>1</sup>H-NMR (300 MHz, CDCl<sub>3</sub>)  $\delta$  7.43 (4H, m, H-2', H-6'), 7.29 (6H, m, H-3', H-4', H-5'), 4.57 (1H, d, J<sub>1,2</sub> = 3.8 Hz, H-1), 4.29 (1H, t, J<sub>3-4</sub> = 1.0 Hz, J<sub>4-5</sub> = 3.3 Hz, J<sub>4-OH4</sub> = 3.6 Hz, H-4), 4.12 (1H, dq, J<sub>4-5</sub> = 3.3 Hz, J<sub>5-6</sub> = 6.3 Hz, H-5), 4.06 (1H, t, J<sub>1,2</sub> = 3.8 Hz, J<sub>2,3</sub> = 3.3 Hz, H-2), 3.85 (1H, m, J<sub>2-3</sub> = 3.3 Hz, J<sub>3-4</sub> = 1.0 Hz, J<sub>3-OH3</sub> = 11.0 Hz, H-3), 2.77 (1H, d, J<sub>3-OH3</sub> = 11.0 Hz, OH-3), 2.02 (1H, d, J<sub>4-OH4</sub> = 3.6 Hz, OH-4), 1.32 (3H, d, J<sub>5-6</sub> = 6.3 Hz, H-6). <sup>13</sup>C-RMN (75.4 MHz, CDCl<sub>3</sub>)  $\delta$  133.8 (1C, C-1') 133.4 (1C, C-1') 133.1 (2C, C-2', C-6'), 132.9 (2C, C-2', C-6'), 129.1 (2C, C-3', C-5'), 129.1 (2C, C-3', C-5'), 128.3 (2C, C-4', C-4'), 87.2 (1C, C-2), 81.3 (1C, C-4), 79.7 (1C, C-3), 77.7 (1C, C-5), 62.2 (1C, C-1), 13.3 (1C, C-6). EM-IE *m/z* 347 [M + H]<sup>+</sup> (1), 231 (10), 203 (20), 177 (100), 135 (5), 109 (24), 91 (9), 45 (13).

### 2.5 Bioassay Toxicity in the *Artemia salina* Model

Cysts of *Artemia salina* (200 mg) were disinfected using a 1 % hypochlorite solution, deposited in a container of 20 × 20 × 30 cm with 250 mL of saltwater (20 g L<sup>-1</sup> of salt), at 37 °C. The optimum hatching percentage was obtained after 72 h. Nauplii of *A. salina* were placed in tubes of 15 mL. To optimize the harvest, suitable conical cylinders were used to favour the movement of the nauplii towards the light. Finally, the compound was evaluated by triplicate with five different concentrations (100, 10, 1, 0.1, 0.01  $\mu\text{g mL}^{-1}$ ).<sup>17,18</sup>

### 3. Results and Discussion

The synthesis of diphenylacetals **2** and **6**, derived from L-fucose (**1**) and L-rhamnose (**5**), respectively, was carried out by using the reaction reported by Frago-Serrano *et al.* in 2001.<sup>1</sup> The resulting compounds were purified by normal-phase column chromatography.

The obtained diphenylacetals were reacted with tosyl chloride in pyridine. In the case of diphenyl-dithiol **6**, derived from

L-rhamnose (**5**), the cyclic compound **8** was obtained with a yield nearing 80 %, whereas in the case of diphenyl-dithiol **2**, derived from L-fucose (**1**), the tosylated compound **3** was obtained with a yield close to 50 %. The structure of compounds **3** and **8** was determined by one- and two-dimensional nuclear magnetic resonance (NMR) techniques. The chemical shift values and proton-proton coupling constants are described in the experimental part.

With the aim of establishing the difference in reactivity of diphenyl-dithiols **2** and **6**, conformational analyses of the tosylated product **3** from L-fucose (**1**) and of the theoretical tosylate product **7** from L-rhamnose (**5**) were performed. The theoretical tosylate **7** is proposed as a possible intermediary for the formation of cyclic compound **8** (Fig. 2). Both conformational analyses were carried out using the Monte Carlo method.<sup>19,20</sup>

The conformers obtained with the Monte Carlo search method were optimized by employing MMFF. These models only consider steric interactions and electrostatic effects but do not consider electronic lone pairs and other electronic effects.<sup>16</sup> The geometry of the conformers was optimized by using the calculation base AM1. The AM1 method is located at a semi-empirical level of theory, it uses parameters derived from crystallographic data, and includes considerations on some electronic effects. This later conformer distribution was optimized using the hybrid DFT hybrid method using B3LYP and the DGDZVP basis set (B3LYP/DGDZVP). The geometries and theoretical formation energies were compared.

The conformational space sampling of compound **3** shows a relatively narrow distribution at equilibrium. The optimization of the conformer distribution with AM1 method shows a different global minimum, respectively, of MMFF method. The AM1 optimized conformers were submitted to DFT/B3LYP/DGDZVP optimization. Table 1 exhibits the low flexibility of compound **3**, only five conformers calculated from the original MMFF distribution contribute to the equilibrium. The global minimum at DFT level shows an intramolecular bond between the hydroxyl group in the position 4 of the chain and the SO group in position 5. This hydrogen bond stabilizes the conformation and forms a seven-member ring in this molecule.

The conformer distribution for compound **3** is wider than the one found for compound **7**. It is necessary to consider that the MMFF and AM1 levels do not calculate polarization effects through the space and only take in account the torsional energy, the steric hindrance and lone-pair effects, and as a consequence, the calculation produces a larger conformer distribution. At the DFT level, the conformer distribution is reduced to only four contributing conformers (Table 2). The global minimum is stabi-

**Table 2** Minimum energy conformers of the proposed intermediary 7 derived from L-rhamnose (5), obtained by the Monte Carlo method combined with MMFF and re-optimized by employing the semi-empirical calculation base AM<sub>1</sub> and DFT method B3LYP/DGDZVP. The global minimum of each theory level distribution is in italics.

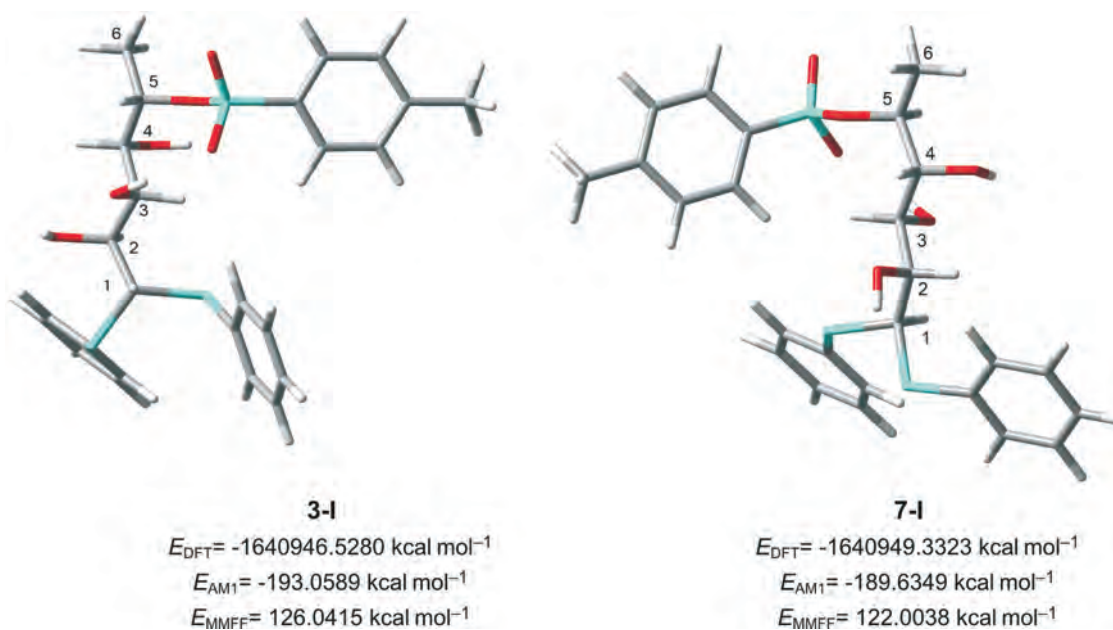
Conformer	$E_{\text{MMFF}}/\text{kcal mol}^{-1}$	$P_{\text{MMFF}}$	$E_{\text{AM1}}/\text{kcal mol}^{-1}$	$P_{\text{AM1}}$	$E_{\text{DFT}}/\text{kcal mol}^{-1}$	$P_{\text{DFT}}$
7-I	122.0038	0.1037	-189.6349	0.0008	-1640949.3323	0.9836
7-II	124.1672	0.0027	-189.6917	0.0009	-1640946.8624	0.0152
7-III	123.7761	0.0052	-189.7872	0.0010	-1640945.0201	0.0007
7-IV	123.6861	0.0061	-192.1643	0.0551	-1640944.5538	0.0003
7-V	123.4462	0.0091	-191.5381	0.0192	-1640943.4526	0.0000
7-VI	123.0031	0.0192	-189.8064	0.0010	-1640943.4149	0.0000
7-VII	126.4424	0.0001	-189.5402	0.0007	-1640943.2662	0.0000
7-VIII	122.3291	0.0599	-189.5049	0.0006	-1640943.2154	0.0000
7-IX	122.5798	0.0392	-193.3678	0.4199	-1640942.7316	0.0000
7-X	121.5982	0.2056	-192.9965	0.2244	-1640942.4197	0.0000
7-XI	124.7096	0.0011	-189.9422	0.0013	-1640941.9095	0.0000
7-XII	126.4067	0.0001	-191.5639	0.0200	-1640941.2870	0.0000
7-XIII	123.8788	0.0044	-190.5066	0.0034	-1640941.1113	0.0000
7-XIV	125.5129	0.0003	-192.3138	0.0709	-1640940.3163	0.0000
7-XV	126.2681	0.0001	-192.5819	0.1115	-1640940.1274	0.0000
7-XVI	121.0228	0.5427	-190.8356	0.0059	-1640940.0929	0.0000
7-XVII	126.6992	0.0000	-191.7151	0.0258	-1640939.4196	0.0000
7-XVIII	125.2621	0.0004	-191.1347	0.0097	-1640938.9954	0.0000
7-XIX	126.5166	0.0001	-191.3253	0.0134	-1640937.4203	0.0000

lized by the formation of an eight-member ring by an intramolecular bond between the hydroxyl group in position 3 and the SO group in the position 5.

Tables 1 and 2 show the obtained conformers, as well as, their participation in the equilibrium calculated by their formation enthalpy.<sup>1-2</sup> The conformational analysis at MMFF and AM1 highlights the fact that the by-product proposed as the intermediary 7 of L-rhamnose shows a more subtle mobility than that of compound 3 derived from L-fucose. In the case of this latter, the conformer in zig-zag geometry represents over 99 % at equilibrium using molecular mechanics and semi-empirical methods the same results were obtained when the DFT calculation was applied. In the case of intermediary 7, the semi-empirical method indicates that, in the conformational space, there is a mixture of three main conformers (Table 2); this mobility does

not correlate using DFT/B3LYP/DGDZVP calculation. If we examine the minimum energy conformer for 7, we notice that the steric and electrostatic arrangements induces a conformation that favours the cyclization reaction and the formation of compound 8. The hydroxyl group at the carbon 2 position is in a plane opposite to that of the hydroxyls at carbons 3 and 4, as is shown in Fig. 3; moreover, the intermediary tosylate has a configuration suitable for the cyclization reaction, thus favouring the formation of compound 8. On the other hand, in the case of 3, the hydroxyl group of carbon 2 of the global minimum DFT conformer exhibits electrostatic interaction with the hydroxyl of carbon 3 (Fig. 3) and, because both hydroxyl groups are in the same plane, they also present steric hindrance between them. These interactions avoid the cyclization of compound 3.

Additionally, the calculated conformer distribution of 3

**Figure 3** Comparison of the global minima DFT conformers of compounds 3 and 7, derived from L-fucose and L-rhamnose, respectively. The energies at different theory levels are lower for the minimum of derivative 7. In the model of conformer 3-I, the hydroxyl in C3 hinders the cyclization, thus compound 4 is not favoured (according with the reaction scheme in Fig. 2).

**Table 3** Theoretical coupling constants (Hz) of the main conformers of product 3. These values validate the experimental conformer distribution.

Conformer	<i>P</i>	<i>J</i> <sub>1-2</sub>	<i>J</i> <sub>2-3</sub>	<i>J</i> <sub>3-4</sub>	<i>J</i> <sub>4-5</sub>
3-I	0.4649	11.3	0.9	9.4	1.2
3-II	0.4226	11.3	0.9	9.4	1.2
3-III	0.0395	11.6	1.0	9.2	1.3
3-IV	0.0350	1.9	8.7	9.4	1.4
3-V	0.0327	2.6	0.5	9.8	0.8
DGDZVP weighted <i>J</i> values		10.6	1.2	9.4	1.2
Experimental <i>J</i> values		7.9	1.4	9.3	1.0

**Table 4** Distance between the hydroxyl group in carbon 2 and the carbon 5 of the most stable DFT conformers for the compounds 3 and 7.

Conformer	<i>P</i>	<i>d</i> /Å	Conformer	<i>P</i>	<i>d</i> /Å
3-I	0.4649	4.318	7-I	0.9836	4.264
3-II	0.4226	4.325	7-II	0.0152	4.186
3-III	0.0395	4.318	7-III	0.0007	4.321
3-IV	0.0350	4.964	7-IV	0.0003	4.240

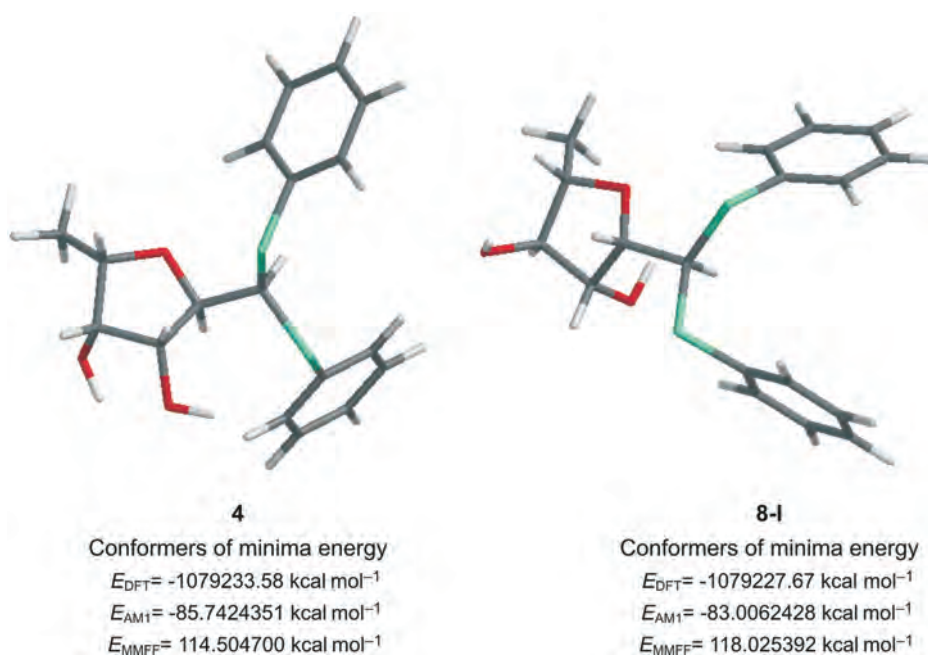
optimized by B3LYP/DGDZVP agrees with the experimental conformation reflected by the coupling constants in CDCl<sub>3</sub> at 300 MHz, proving that the conformations found *in silico* are credible, and that the method is valid (Table 3).

Another piece of information that supports the stability of compound 3 and the cyclization of the proposed intermediary 7, is the distance between the oxygen of the hydroxyl groups at carbon 2 and carbon 5 of the tosylate (Table 4). When the global minima were compared, it was found that the distance in the case of the derivate of L-rhamnose (4.264 Å) is moderately shorter than that in the case of the derivate of L-fucose (4.318 Å), which indicates an increased probability for the occurrence of the cyclization reaction in 7. The analysis of the NOE spectrum of 3 reveals interactions of H-1 with H-2 and H-3; the interactions of H2 are with H-1, H-3 and H-4; the atom H-3 interacts with H-1, H-2, H-4 and H-5; H-4 interacts with H-5 and H-6.

These data support the evidence of a zig-zag conformation of the L-fucose chain in the derivative 3.

These observations corroborate the addition of the tosylate in position 5 forming the main product for the derivative of L-fucose, and the cyclical compound for the case of L-rhamnose, with the formation of the intermediary tosylate 7.

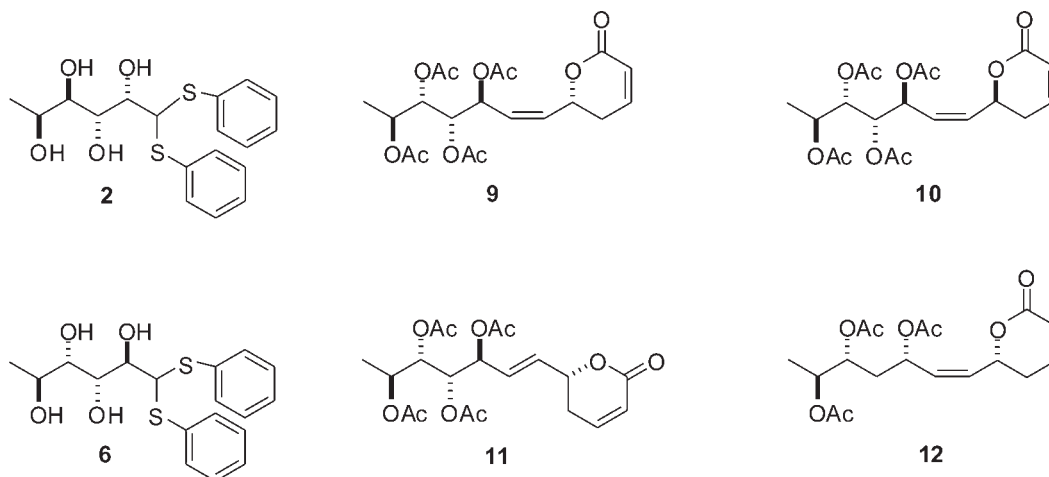
In the method described above for 3 and 7 in the conformational analysis of 4 and for 8, we found that the cyclic derivative 4 is more stable than cycle 8 (Fig. 4); however, cycle compound 4 is not formed in the reaction as explained earlier. It is important to mention that the conformational analysis was corroborated using the comparison between the experimental and the theoretical coupling constants (Table 5). This comparison shows that the conformers that were found are representative of the compounds in solution, due to the similarity between the coupling constants, experimental and theoretical.

**Figure 4** Energy comparison between the theoretical furanoside cycle of L-fucose 4 and L-rhamnose 8.

**Table 5** Theoretical coupling constants (Hz) of the main conformers of product 8. These values validate the experimental conformer distribution.

Conformer *	$E_{\text{DFT}}/\text{kcal mol}^{-1}$	$P$	$J_{1-2}$	$J_{2-3}$	$J_{3-4}$	$J_{4-5}$
8-I	-1079227.67	0.6195	1.2	3.8	0.2	1.1
8-II	-1079227.33	0.3805	11.1	2.6	0.2	3.3
DGDZVP weighted $J$ values			4.9	3.3	0.2	1.9
Experimental $J$ values			3.8	3.3	1.0	3.3

\* The analysis conformational was carried out employing the methodology described for compounds 3 and 7.

**Figure 5** Similarity of compounds 2 and 6 with spicigerolide (9) and compounds 10–11.

The results of this study demonstrates that it is feasible to explain the reactivity of highly flexible compounds by means of conformational analysis, combining a stochastic search protocol using the Monte Carlo simulation approach, with an optimization at a high theory levels *via* semi-empirical methods, such as the calculation base AM1 and subsequently refining the conformers using DFT method.

In addition, the toxicity of compounds 2 and 6 was evaluated due the similarity in the side chain of the cytotoxic derivatives of sugars such as pironetin and other cytotoxic 6-heptenil-5,6-dihydro-2*H*-piran-2-ones (Fig. 5). This cytotoxicity property can be monitored using the brine shrimp (*Artemia salina*) assay. In this study the values found are in the range 100–1000  $\mu\text{g mL}^{-1}$  (Table 6), indicating that the toxicity levels of compounds 2 and 6, are not suitable to carry out further, more advanced, *in vitro* pharmacological tests.<sup>21</sup>

#### 4. Conclusions

The conformational analysis of the diphenylacetals 3 and 7 using computational chemistry methods explains the mechanism for the formation of 8, *via* the spontaneous cyclization of the proposed intermediary 7, in contrast to obtaining the open monotosylate 3 from L-fucose (1).

**Table 6** Toxicity assay (*Artemia salina*).

$\mu\text{g mL}^{-1}$	Blank	2	6	Tymol *
0.001	0	0	0	0
0.1	0	0	0	5( $\pm$ 5)
1	0	0	0	50( $\pm$ 3)
10	7( $\pm$ 3)	0( $\pm$ 3)	0( $\pm$ 3)	57( $\pm$ 3)
100	10( $\pm$ 3)	33( $\pm$ 9)	30( $\pm$ 4)	87( $\pm$ 7)
1000	3( $\pm$ 3)	56( $\pm$ 8)	50( $\pm$ 2)	98( $\pm$ 4)

\* Tymol was employed with positive control.

These kinds of methods can be used to study the differences in reactivity of highly flexible compounds. The cyclization reaction observed represents a potentially useful chemical alternative for the synthesis of cycles of the furanoside type. Despite the low cytotoxic activity of compounds 2 and 6 (measured indirectly in *Artemia* sp. nauplii), these compounds can be used as construction blocks for the development of substances with antiviral activity, such as the nucleoside analogues.

#### References

- R. Pereda-Miranda, M. Fragoso-Serrano and C.M. Cerda-García-Rojas, *Tetrahedron*, 2001, 57, 47–53.
- J.A. Mendoza-Espinoza, F. López-Vallejo, M. Fragoso-Serrano, R. Pereda-Miranda and C.M. Cerda-García-Rojas, *J. Nat. Prod.*, 2009, 72, 700–708.
- M.A. Sarotti and C.S. Pellegrinet, *J. Org. Chem.*, 2009, 74, 7254–7260.
- G.S. Smith and M.J. Goodman, *J. Org. Chem.*, 2009, 74, 4597–4607.
- T. Hirokawa, *Bio. Industry*, 2008, 25, 62–69.
- M.F. Lensink and R. Méndez, *Curr. Pharm. Biotechnol.*, 2008, 9, 77–86.
- S. Achmad, T. Hoyer, A. Kjaer, L. Makmur and R. Norrestam, *Acta Chem. Scand.*, 1987, B41, 599–609.
- A. Alemany, C. Márquez, C. Pascual, S. Valverde, A. Perales, J. Fayos and M. Martínez-Ripoll, *Tetrahedron Lett.*, 1979, 37, 3579–3582.
- J. García-Fortanet, J. Murga, M. Carda and J.A. Marco, *ARKIVOC*, 2005, 9, 175–188.
- R. Pereda-Miranda, L. Hernández, M.J. Villavicencio, M. Novelo, P. Ibarra, H. Chai and J.M. Pezzuto, *J. Nat. Prod.*, 1993, 56, 583–93.
- M. Fragoso-Serrano, S. Gibbons and R. Pereda-Miranda, *Planta Med.*, 2005, 71, 278–280.
- E. Falomir, J. Murga, P. Ruíz, M. Carda, J.A. Marco, R. Pereda-Miranda, M. Fragoso-Serrano and C.M. Cerda-García-Rojas, *J. Org. Chem.*, 2003, 68, 5672–5676.
- H. Nagata, T. Usui, S. Kobayashi, K. Tsuchiya and K. Nishikawa, Japan Patent, 1999, JP 11001434 A.
- T. Usui, H. Watanabe, H. Nakayama, Y. Tada, N. Kanoh, M. Kondoh, T. Asao, K. Takio, H. Watanabe, K. Nishikawa, T. Kitahara and H. Osada, *Chem. Biol.*, 2004, 11, 799–806.

- 15 J.E. Peralta, G.E. Scuseria, J.R. Cheeseman and M.J. Frisch. *Chem. Phys. Lett.*, 2003, **375**, 452–258.
- 16 V. Sychrovskĕ, J. Gräfenstein and D. Cremer. *Chem. Phys.*, 2000, **113**, 3530–3547.
- 17 B.N. Meyer, N.R. Ferrigni, J.E. Putnam, L.B. Jacobsen, D.E. Nichols and J.L. McLaughlin, *Planta Medica*, 1982, **45**, 31–34.
- 18 W. Voigt, *Methods Mol. Med.*, 2005, **110**, 39–48.
- 19 R. Mannhold, H. Kubinyi and H. Timmerman, Methods and principles in medicinal chemistry, in *Molecular Modeling. Basic Principles and Applications*, (H.D. Höltje and G. Folkerts, eds.), vol. 5, VCH, Weinheim, 1996, pp. 23–36.
- 20 C.A.G. Haasnoot, F.A.A.M. De Leeuw and C. Altona, *Tetrahedron*, 1980, **36**, 2783–2792.
- 21 P. Skehan, R. Storeng, D. Scudiero, A. Monks, J. McMahon, D. Vistica, J.T. Warren, H. Bokesch, S. Kenney and M.R. Boyd, *J. Natl. Cancer Inst.*, 1990, **82**, 1107–1112.